



Earth Pressure Distribution on Buried Pipes Installed with Geofoam Inclusion and Subjected to Cyclic Loading

Mohamed A. Meguid¹ · Mahmoud R. Ahmed¹

Received: 6 November 2019 / Accepted: 20 January 2020
© Springer Nature Switzerland AG 2020

Abstract

Buried pipes and culverts installed under embankments supporting transport infrastructure are often designed to carry both static and cyclic loading. Earth pressures acting on these structures are affected by the installation conditions. The induced trench approach is used to reduce the contact pressure on rigid culvert's walls under heavy embankments by utilizing the shear strength within the backfill. A compressible material, such as the EPS geofoam blocks, is generally placed above the buried structure and the overlying prism of soil is allowed to move downward. In this work, the distribution of the contact pressure on a pipe buried within granular material and experiencing cyclic loading is investigated. Results are presented at key locations on the pipe circumference and the changes in contact pressure during cyclic loading are examined. Results show that the installation of EPS geofoam block over the pipe resulted in overall enhanced performance of the soil–geofoam–pipe system with significant reduction in the measured radial pressure, particularly at the crown and invert locations. Less pronounced effect was found at the sides of the pipe. These results confirmed that the inclusion of EPS geofoam within the backfill material can significantly enhance the response of buried structures particularly for shallow-buried pipes under repeated loading.

Keywords Contact pressure measurement · Buried pipes · Cyclic loading · Induced trench · EPS geofoam

Introduction

Earth loads on buried pipes and culverts are dependent on several factors, among which are the installation conditions. Conduits are usually installed in a trench which is located under the natural ground surface. Frictional forces, between the trench sides and the backfill, contribute to supporting the weight of the overlying soil. In contrast, embankment installation represents a case where the soil is constructed layer-by-layer above the natural ground. This results in higher vertical earth pressures on the buried structure. The induced trench installation is conventionally used to reduce the vertical load on rigid conduits. This method is based on the deployment of a compressible layer directly above the conduit to generate positive arching within the covering soil.

The specifications of the Canadian highway [1] and the AASHTO LRFD bridge design [2] provide general guidelines to estimate the earth pressures on positive projecting culverts; however, no guidance is found for the induced trench technique. Although induced trench construction technique has been utilized for decades to reduce the earth loads on rigid conduits installed under heavy embankments, the feasibility of this method has become questionable to many designers [3]. The induced trench installation method for rigid conduits in high embankments environment has been used since the early twentieth century. More recent studies have investigated this soil–structure interaction problem using laboratory and field experiments [4–13], as well as numerical analysis [14–19] in attempts to understand the effectiveness of this construction technique and address the uncertainties associated with this design.

This experimental study aims to understand the response of small pipes installed in granular material with geofoam inclusion and subjected to repeated loading. A thick-walled pipe with tactile sensors is installed in granular backfill under controlled environment. The cyclic loading

✉ Mohamed A. Meguid
mohamed.meguid@mcgill.ca

Mahmoud R. Ahmed
mahmoud.ahmed@mail.mcgill.ca

¹ Department of Civil Engineering and Applied Mechanics,
McGill University, Montreal, QC, Canada

considered in the study is applied at the surface along the pipe's centerline.

The paper is organized as follows: the description of the experimental setup and conducted tests are presented in Sect. 2, followed by a brief description of the response of the pipe under three loading–unloading cycles. The measured pressures are compared for the cases of embankment installation (no compressible material) and induced trench installation (ITI) with EPS block introduced above the pipe.

Experimental Investigation

The tests are performed in a strong chamber that hosts both the buried pipe and the granular backfill. A stiff pipe of a relatively thick wall is instrumented and buried within the backfill soil. Before the pipe installation, tactile sensing sheets were taped directly to the outer circumference of the pipe. A strip load attached to a universal MTS press machine is used to apply the cyclic loading at the soil surface, as depicted in Fig. 1.

Strong Chamber

The dimensions of the chamber are 1.4 m in width and 1 m in height with 0.45 m in depth to fit the length of the pipe (see Fig. 1). These dimensions are selected to resemble 2D loading condition. To reduce the rigid boundary effects, the distance between the rigid walls and the pipe is optimized with respect to the pipe diameter. The distance between the chamber's sidewalls and the pipe is 0.65 m and that is four times the pipe's diameter.

All the surfaces of the steel walls are covered using a thin epoxy coating. Two sheets of plastic, with a thin

grease layer in between, are then attached to cover the inner sides. The grease layer is conventionally used to reduce the effect of friction between the backfill and the walls.

Instrumented Thick-Wall Pipe

A high-density PVC pipe is placed at a depth of 0.45 m below the soil surface. The pipe used is 15 cm in inner diameter and 1 cm in wall thickness, as shown in Fig. 2. Two Tact Array pressure-sensing sheets are attached to the surface of the pipe [20]. Additional details regarding the instrumented pipe are given elsewhere [9–11, 21].

The sensing sheets are calibrated by the manufacturer and tested in the laboratory in preparation for this study. The sheets are tested on a flat surface as well as curved surface. This is done using two different types of wooden frames. The first had rectangular-shaped walls, while the second included half-circular cuts made on two opposite walls to fit over the instrumented pipe. Gravel material of 2 kg in mass are then introduced the sheets and data acquisition system is used to measure the earth pressure. For the two considered cases, the readings of the data acquisition systems matched the applied loads and showed reliable performance. Further details of the sensor calibration and performance can be found in previous publications [10, 21].

Although the pipe stiffness is chosen to minimize deformation under the maximum applied surface pressure (140 kPa), additional measures are considered to support this assumption. This is done by measuring the diametrical change using two LVDTs placed orthogonally inside the pipe. The highest recorded variation in the diameter was found to be less than 0.05 mm at the mentioned pressure, which is negligible.

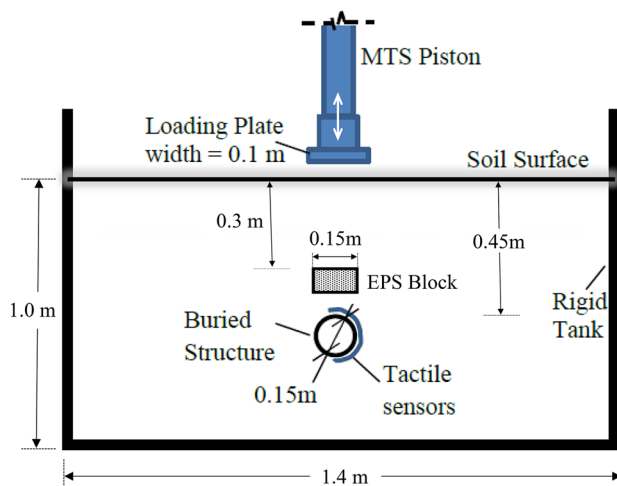


Fig. 1 Test setup used to perform the experiments

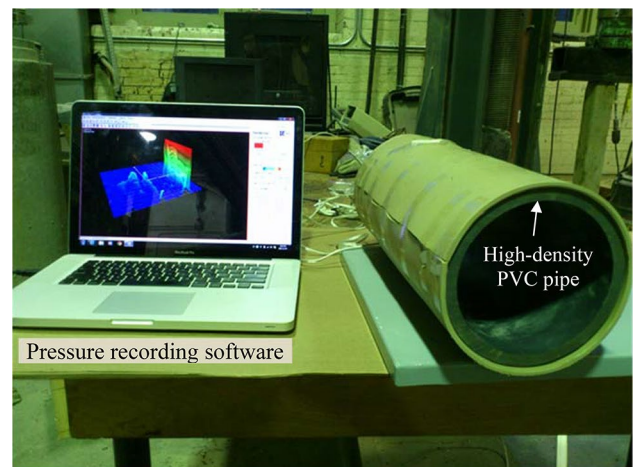


Fig. 2 Instrumented pipe and pressure recording software

Properties of the EPS and Backfill Materials

Before commencing the test program, compressive strength tests are conducted on 100 mm cubical EPS samples according to the specifications of ASTM D1621-10 [22]. The results, depicted in Fig. 3a, show that EPS experienced strain hardening response with linear relationship between axial strain and compressive strength up to 1% strain. Table 1 summarizes the properties of EPS22 compressive strength at 1%, 5%, and 10% strain.

The shear strength parameters are obtained using direct shear tests performed on a 100 mm × 100 mm samples. The tests included three applied normal stresses: 18 kPa, 36 kPa, and 54 kPa [23]. The horizontal displacement and the associated shear stresses are shown in Fig. 3b. The results show that shear stresses generally increased with the increase

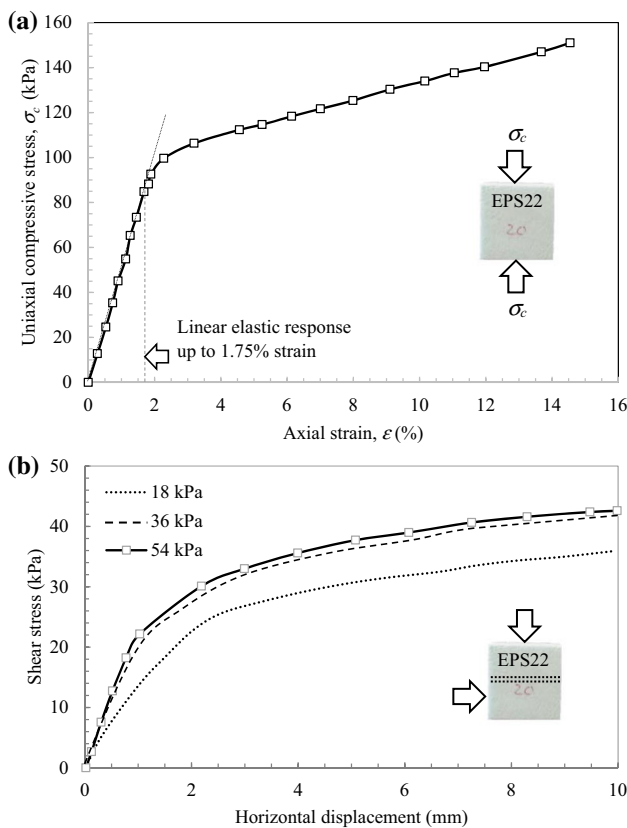


Fig. 3 Determining the properties of the geofoam material: **a** uniaxial compression; and **b** direct shear tests

Table 1 Uniaxial compressive strength data of EPS22

% of the measured value	100%	50%	10%
Uniaxial compressive strength (kPa) at 1% deformation	50	25	5
Uniaxial compressive strength (kPa) at 5% deformation	115	57.5	11.5
Uniaxial compressive strength (kPa) at 10% deformation	135	67.5	13.5

in geofoam density for the applied range of horizontal displacements.

Particle-size distribution of the backfill material (dry sandy gravel) is established using sieve analysis performed on representative soil samples. The granular material consists of 23% sand and 77% gravel as shown in the particle-size distribution given in Fig. 4. Direct shear tests are used to determine the backfill friction angle for normal stresses that range between 10 and 40 kPa. Assuming linear failure envelope, the friction angle is found to be 44°. The material properties are given in Table 2.

Test Procedure

The soil placement steps described above are used throughout this study. This ensures consistent initial conditions in all tests. Four experiments were conducted: two with only the instrumented pipe within the backfill material (benchmark tests) and two tests that include EPS geofoam inclusion. The soil is added incrementally and tamped in place to ensure dense bedding underneath the pipe. The pipe is then placed above a thin layer of sand to enhance the interaction of the pipe with the bedding soil and avoid potential damage to the sensing sheets. The backfill is added in layers to cover the pipe with 0.45 m, which corresponds to a total soil height of 1.0 m. Density cups are placed at different locations in the chamber to measure the backfill density. The thickness of the EPS block is chosen to be around 50% of the pipe diameter [5, 16].

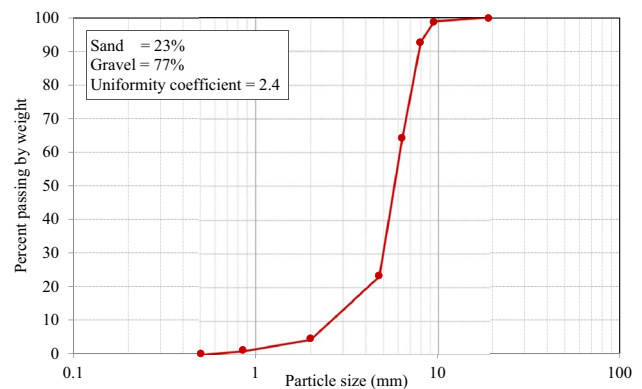


Fig. 4 Particle-size distribution of the backfill material

Table 2 Properties of the backfill material

Property	Value
Specific gravity	2.65
D_{60}	6.2 mm
D_{30}	5 mm
D_{10}	2.6 mm
Coefficient of uniformity (C_u)	2.4
Coefficient of curvature (C_c)	1.6
Minimum dry unit weight (γ_{min})	15.1 kN/m ³
Maximum dry unit weight (γ_{max})	17.3 kN/m ³
Experimental unit weight (γ_d)	16.3 kN/m ³
Internal friction angle (ϕ)	44°

Surface load is applied via a steel plate that measures 45 cm in length and 10 cm in width. The plate is placed at the soil surface along the centerline of the pipe and connected to the MTS actuator. The cyclic load is applied at a rate of displacement of 1.3 mm/min. Three loading and unloading cycles are applied and the corresponding contact pressures on the pipes are recorded. The tests are stopped in one of the following cases: (1) the surface displacement reaches 22 mm; or (2) the measured pressure reached the capacity of the sensors (140 kPa). At the end of each test, the steel chamber is cleared from the backfill soil using a vacuum system and the pipe is recovered. Figure 5 shows the distribution of the radial pressure measured using the data acquisition system before surface loading is applied.

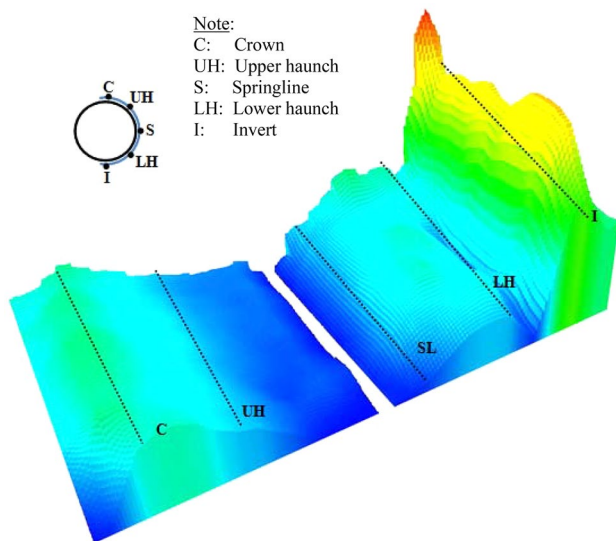


Fig. 5 A sample of the measured pressure distribution around the pipe circumference

Initial Distribution of Pressure on the Pipe

The initial pressure on the pipe for the benchmark tests (without EPS geofoam) is shown in Fig. 6. The pressure measured at the invert, spring line, and crown were found to be 40, 8, and 12 kPa, respectively. These pressures are consistent with the negative arching that develops due to the installation of a rigid pipe using the embankment construction method over compacted bedding material. The results are also consistent with Hoeg’s theoretical solution [24] that predicts the radial earth pressure at the crown, expressed by Eq. (1):

$$\sigma_r = \frac{1}{2}p \left\{ (1+k) \left[1 - a_1 \left(\frac{R}{r} \right)^2 \right] - (1-k) \left[1 - 3a_2 \left(\frac{R}{r} \right)^4 - 4a_3 \left(\frac{R}{r} \right)^2 \right] \cos 2\theta \right\} \quad (1)$$

The constants are defined by the following equations for the fully bonded interface case:

$$a_1 = \frac{(1-2\nu)(C-1)}{(1-2\nu)C+1} \quad (2)$$

$$a_2 = \frac{(1-2\nu)(1-C)F - \frac{1}{2}(1-2\nu)^2C + 2}{[(3-2\nu) + (1-2\nu)C]F + \left(\frac{5}{2} - 8\nu + 6\nu^2\right)C + 6 - 8\nu} \quad (3)$$

$$a_3 = \frac{[1 + (1-2\nu)C]F - \frac{1}{2}(1-2\nu)C - 2}{[(3-2\nu) + (1-2\nu)C]F + \left(\frac{5}{2} - 8\nu + 6\nu^2\right)C + 6 - 8\nu} \quad (4)$$

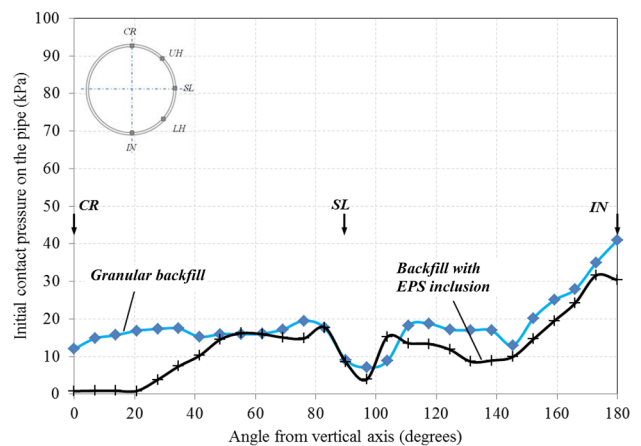


Fig. 6 Initial pressure distribution acting on the pipe

Here, ν = The medium Poisson’s ratio; k = The lateral pressure factor = $\nu / (1 - \nu)$; R = The pipe radius; r = The distance from the pipe center to the medium soil element; C = The Compressibility ratio; and F = The Flexibility ratio.

where C and F are the stiffness ratios needed to express the relative stiffness between the conduit and the soil calculated as follows:

$$C = \text{compressibility ratio} = \left(\frac{1}{2}\right) \frac{1}{1 - \nu} \frac{M^*}{E_c} \left(\frac{D}{t}\right) \tag{5}$$

$$F = \text{flexibility ratio} = \left(\frac{1}{4}\right) \frac{1 - 2\nu}{1 - \nu} \frac{M^*}{E_c} \left(\frac{D}{t}\right)^3, \tag{6}$$

in which: M^* = the constrained modulus; E_c = the conduit Young’s modulus; D = pipe diameter; t = Pipe wall thickness; and ν_c = the conduit Poisson’s ratio.

A summary of the soil and pipe parameters used to calculate earth pressure at the crown ($\theta=0^\circ$) is provided in Table 3. The calculated radial pressure at the crown using Hoeg’s solution is found to be about 9 kPa. Although the calculated pressure is lower than that measured in the experiment (12 kPa), it is considered acceptable, as the measured radial pressure is generally sensitive to soil placement process above the pipe.

Figure 6 also shows the distribution of the contact pressure for the case of geofoam block installed above the pipe. The presence of the geofoam layer is found to cause redistribution of the earth pressures acting on the pipe with significant reduction in pressure at the crown (0°) and the upper portion of the pipe circumference (up to 40° from the crown). Less pronounced change in radial pressure was measured on the lower half of the pipe. The pressure at the invert was found to be sensitive to the compaction of the bedding layer, with maximum pressure value of 40 kPa. After the installation of the geofoam, the initial pressure at both the crown and invert locations decreased by about 10 kPa. This presents a reduction of more than 90% at the crown and about 25% at the invert.

Table 3 Parameters used to calculate initial pressure on the pipe using Hoeg’s solution

Parameters				
Pipe	I.D (m)	t (mm)	E_c (GPa)	ν_c
	0.15	0.1	200	0.28
Soil	γ (kN/m ³)	C	M^* (MPa)	ν
	16.3	0.01	150	0.35

It has been noted that the difference in pressure at the crown and invert (about 28 kPa) is equivalent to the contact pressure measured due to the self-weight of the pipe (in air). This observation is true for both initial and maximum loading conditions and confirms that, despite the sensitivity of the pressure distribution to the pipe placement procedure, the sensors are able to read the net pressure induced by the backfill material with reasonable accuracy.

Effect of Cyclic Loading

The measured radial pressures at different locations on the pipe due to the applied cyclic loading are summarized in Table 4. Details of the measured responses are given below.

At the Crown (0°)

Before the geofoam is introduced, the initial radial pressure at the crown was found to increase from 12 to 88 kPa when the surface pressure increased from 0 to about 200 kPa as illustrated by the solid line in Fig. 7. At the end of the first cycle, where the surface load is brought back to 1 kPa, the contact pressure decreased from 88 to 62 kPa. On reloading, the maximum contact pressure increased from 88 to 103 kPa in cycle 2 and further increased to 113 kPa in cycle 3. The final pressure at the end of the third cycle was found to be 84 kPa which represents a significant residual pressure from the initial pressure of 12 kPa.

After the geofoam block is introduced above the pipe, the initial radial pressure was significantly small as illustrated by the broken line in Fig. 7. At the end of the first loading cycle, the pipe crown experienced insignificant increase in contact pressure from the initial value. Additional two cycles of reloading and unloading resulted in a maximum pressure increase of about 21 kPa.

Comparing the change in final pressure at the crown for the two cases at the end of the three loading cycles reveals a change in pressure from 84 kPa for granular backfill to

Table 4 Measured pressure changes after geofoam installation

Location	Contact pressure (kPa)			
	Initial (before cyclic loading)		After the 3rd loading cycle	
	Granular backfill	With EPS inclusion	Granular backfill	With EPS inclusion
CR (0°)	12	4	84	12
UH (45°)	16	19	28	29
SL (90°)	8	4	9.1	4.8
LH (135°)	18	12	25	21
IN (180°)	17	10	86	58

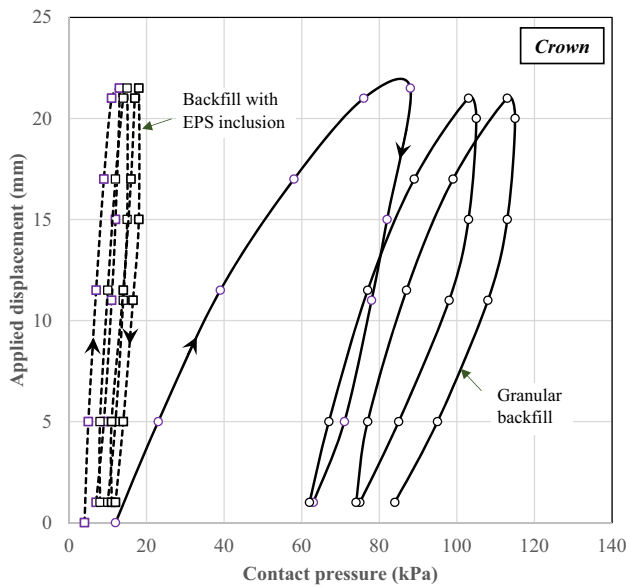


Fig. 7 Effect of cyclic loading on contact pressure at the crown

12 kPa with geofoam inclusion. This corresponds to a pressure reduction at the crown of about 75%.

At the Upper Haunch (45°)

The initial pressure for the case of granular backfill increased from 16 to 28 kPa as the applied surface pressure reached 200 kPa. The solid line in Fig. 8 shows that the maximum contact pressure at the upper haunch did not increase significantly in the second and third loading cycles. The contact

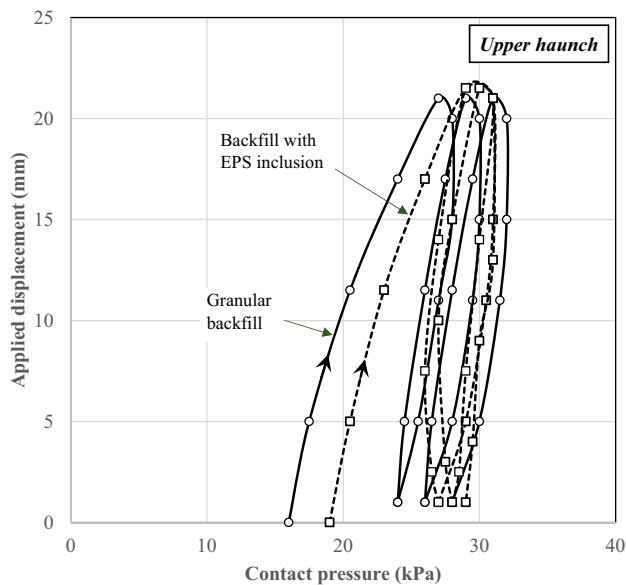


Fig. 8 Effect of cyclic loading on contact pressure at the upper haunch

pressure in the third cycle reached about 32 kPa at the maximum applied pressure and decreased to 28 kPa at the end of the test. This corresponds to a total increase in initial pressure of 12 kPa.

Moreover, the effect from adding the EPS block above the pipe generally induced a slight increase in contact pressure at the upper haunch. This is due to the arching effect of the soil around the pipe and the relative decline of the observed pressure, measured at the pipe’s crown. The change in contact pressure with further loading and unloading was not significant with increase in pressure from 19 kPa at the beginning of the test to 29 kPa after the third loading cycle. This is consistent with Vaslestad et al. [5] who concluded that induced trench installation may result in an increase in lateral earth pressure due to the load re-distribution within the soil.

At the Springline (90°)

The recorded pressure data (Fig. 9) at the springline for the case of granular backfill showed generally low-pressure values (less than 10 kPa). Cyclic loading was found to cause insignificant effect on the contact pressure at the springline. The presence of geofoam was found to generally reduce the contact pressure at the springline. The maximum pressure decreased from about 9 kPa at the maximum applied pressure to about 5 kPa. It was observed that cyclic loading did not have significant effect on the recorded pressures at that location.

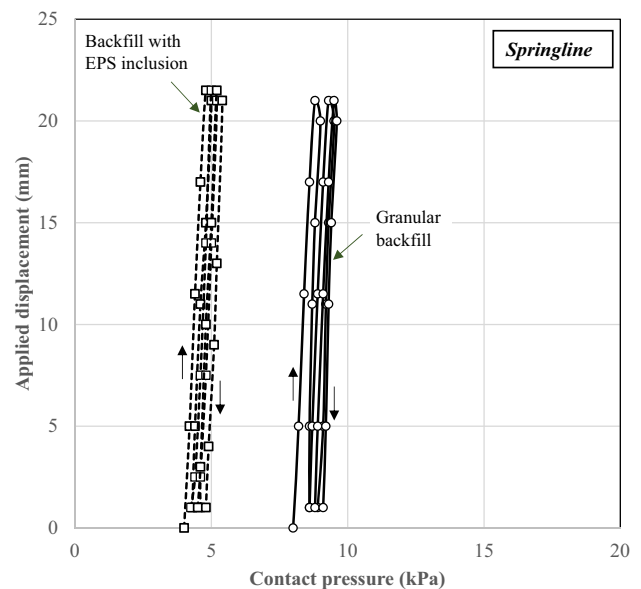


Fig. 9 Effect of cyclic loading on contact pressure at the springline

At the Lower Haunch (135°)

The measured pressure at that location before the geofoam block (the solid line in Fig. 10) is generally higher than that measured at the upper haunch and the springline. A maximum contact pressure of 35 kPa was measured in the third loading cycle at the maximum applied surface pressure. When EPS block was introduced, the maximum pressure decreased to 28 kPa.

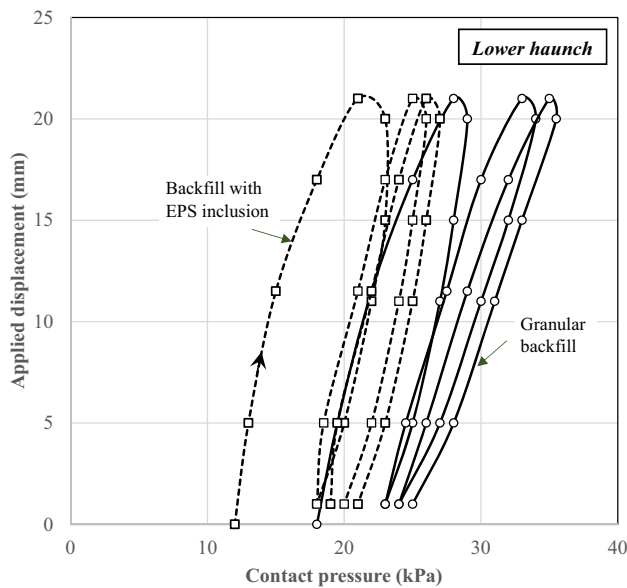


Fig. 10 Development of contact pressure at the lower haunch

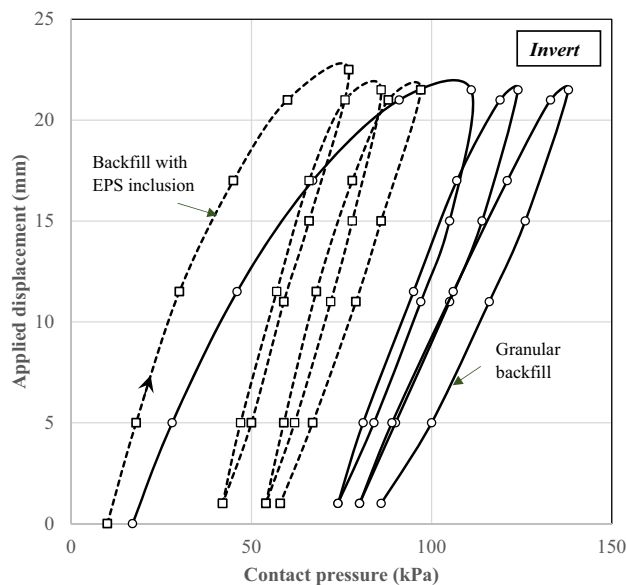


Fig. 11 Development of contact pressure at the invert

At the Invert (180°)

Figure 11 shows the effect of cyclic loading on the contact pressure at the invert. The measured pressure values were generally high compared to those measured elsewhere on the pipe. Before the installation of the geofoam, the maximum contact pressures reached 111 kPa, 124 kPa, and 138 kPa in the first, second and third cycles, respectively. These values decreased to 77 kPa, 86 kPa, and 111 kPa when the geofoam block was installed above the pipe.

A summary of the measured radial pressure at various locations is depicted in Fig. 12. Figure 12a shows the maximum contact pressure at the crown and invert and the cumulative effect of installing EPS block above the pipe due to cyclic loading. Applying cyclic loading with only granular backfill material (indicated by the solid lines) above the pipe resulted in increase in radial pressure at both the crown and invert locations. The presence of geofoam inclusion (shown by the

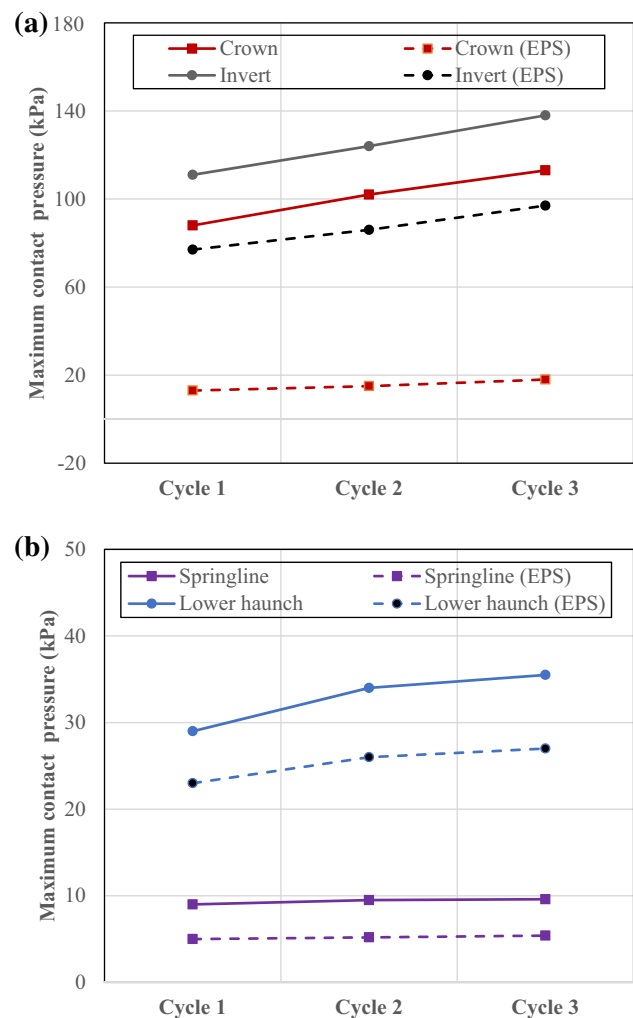


Fig. 12 Changes in contact pressure with the number of cycles: **a** crown and invert; **b** springline and lower haunch

broken lines) resulted in not only a significant reduction in the overall radial pressure but made the effect of cyclic loading less pronounced at the crown. Similar behavior was found at the spring line and lower haunch as illustrated in Fig. 12b. No significant increase in contact pressure at both locations was measured with the increase in the number of loading cycles when a geofoam block was installed above the pipe.

The above response suggests that the inclusion of compressible material above buried structures and the associated soil arching can reduce the load carried by the structure under not only static but also cyclic loading condition as well. Moreover, the above results are obtained using a limited number of loading cycles. More research is, therefore, needed to confirm these results.

Conclusions

For the investigated geofoam density, geometry and backfill material type, the presence of geofoam block resulted in significant reduction in radial earth pressure on the pipe, particularly at the crown location. The upper haunch showed a slight increase in contact pressure due to the positive arching developing within the soil in the vicinity of the pipe. Specific conclusions from this study are given below:

- The final pressure at the crown at the end of the loading cycles decreased from 84 kPa for granular backfill to 12 kPa when geofoam block was installed above the pipe. This corresponds to a pressure reduction at the crown of about 75%.
- The effect was less pronounced along the sides of the pipe with slight reduction in the final pressure at the spring line and lower haunch locations after the completion of the cyclic loading.
- This experimental study suggests that geofoam inclusion can significantly enhance the response of buried pipes particularly for shallow-buried structures under repeatable loading.

Compliance with ethical standards

Funding This study was funded by Natural Sciences and Engineering Research Council of Canada (Grant no. RGPIN-2016-05263).

References

1. CSA (2006) Canadian highway bridge design code—CHBDC. Mississauga, Canada, Canadian Standards Association, p 930
2. AASHTO (2007) American Association of State Highway and Transportation Officials, LRFD Bridge Design Specifications, 4th edn. D.C., USA, Washington
3. McAfee RP, Valsangkar AJ (2008) Field Performance, centrifuge testing, and numerical modelling of an induced trench installation. *Can Geotech J* 45(1):85–101
4. Sladen JA, Oswell JM (1988) The induced trench method—a critical review and case history. *Can Geotech J* 25(3):541–549
5. Vaslestad J, Johansen TH, Holm W (1993) Load reduction on rigid culverts beneath high fills: long-term behavior. *Transp Res Rec* 1415:58–68
6. Liedberg NSD (1997) Load reduction on a rigid pipe: pilot study of a soft cushion installation. *Transp Res Rec* 1594:217–223
7. Sun L, Hopkins T, Beckham T (2011) Long-term monitoring of culvert load reduction using an imperfect ditch backfilled with Geofoam. *Transp Res Rec* 2212:56–64
8. Oshati OS, Valsangkar AJ, Schriver AB (2012) Earth pressures exerted on an induced trench cast-in-place double-cell rectangular box culvert. *Can Geotech J* 49(11):1267–1284
9. Meguid MA, Youssef T (2018) Experimental investigation of the earth pressure distribution on buried pipes backfilled with tire-derived aggregate. *Transp Geotech* 14(1):117–125
10. Meguid MA, Hussein M, Ahmed MR, Omeman Z, Whalen J (2017) Investigation of soil-geosynthetic-structure interaction associated with induced trench installation. *Geotext Geomembr* 45(4):320–330
11. Meguid MA, Ahmed MR, Hussein M, Omeman Z (2017) Earth pressure distribution on a rigid box covered with U-shaped geofoam wrap. *Int J Geosynth Ground Eng* 3(2):1–11
12. Moghaddas Tafreshi SN, Tavakoli Mehrjardi GH, Dawson AR (2012) Buried pipes in rubber-soil backfilled trenches under cyclic loading. *J Geotech Geoenviron Eng* 138(11):1346–1356
13. Sheil BB, Martin CM, Byrne BW, Plant M, Williams K, Coyne D (2012) Full-scale laboratory testing of a buried pipeline in sand subjected to cyclic axial displacements. *Géotechnique* 68(8):684–698
14. Kim K, Yoo CH (2002) Design loading for deeply buried box culverts. highway research center, Report No. IR-02-03. Auburn University, Alabama, USA, p 215
15. Kang J, Parker F, Kang YJ, Yoo CH (2008) Effects of frictional forces acting on sidewalls of buried box culverts. *Int J Numer Anal Meth Geomech* 32(3):289–306
16. McGuigan BL, Valsangkar AJ (2011) Earth pressures on twin positive projecting and induced trench box culverts under high embankments. *Can Geotech J* 48(2):173–185
17. Hazarika H (2006) Stress-strain modeling of EPS geofoam for large-strain applications. *Geotext Geomembr* 24(2):79–90
18. Ekanayake SD, Liyanapathirana DS, Leo CJ (2015) Numerical simulation of EPS geofoam behaviour in triaxial tests. *Eng Comput* 32(5):1372–1390
19. Meguid MA, Hussein MG (2017) A numerical procedure for the assessment of contact pressures on buried structures overlain by EPS geofoam inclusion. *Int J Geosynth Ground Eng* 3(2):1–14
20. Pressure Profile System Inc., Tactarray distributed pressure measurement system. <https://www.pressureprofile.com/tact-array-sensors/>
21. Ahmed M, Tran V, Meguid MA (2015) On the role of geogrid reinforcement in reducing earth pressures on buried pipes. *Soils Found* 5(33):588–599
22. ASTM D1621-10 Standard Test Method for compressive properties of rigid cellular plastics
23. Khan MI, Meguid MA (2018) Experimental investigation of the shear behavior of EPS geofoam. *Int J Geosynth Ground Eng* 4(2):1–12
24. Hoeg K (1968) Stresses against underground structural cylinders. *Am Soc Civ Eng J Soil Mech Found Div* 94(4):833–858

Publisher's Note Springer Nature remains neutral with regard to jurisdictional claims in published maps and institutional affiliations.